JMEPEG (2008) 17:326–329
DOI: 10.1007/s11665-008-9221-9

1059-9495/$19.00

The Upper Limit of Energy Density of Nanoporous Materials Functionalized Liquid

Aijie Han, Venkata K. Punyamurtula, Taewan Kim, and Yu Qiao

(Submitted October 29, 2007; in revised form January 29, 2008)

In this article, we report the experimental result of energy dissipation of a mobil crystalline material (MCM) 41 in mercury. The MCM41 contains a large volume fraction of nanometer-sized pores. As the applied pressure is relatively high, the nanopore surfaces are exposed to mercury. Due to the large nanopore surface area and the large solid-liquid interfacial tension, the energy dissipation effectiveness of this system is ultrahigh, representing the upper limit that can be achieved by the pressure-induced infiltration technique.

Keywords mechanical testing, structural ceramics, surface engineering

1. Introduction

For many decades, people have been actively investigating high-performance energy absorption materials (EAM) (Ref 1), so as to develop lightweight and/or small-sized protective and damping devices, such as car bumpers, buffer systems, and protection layers. Conventional EAM include polymers, composite materials, shape memory alloys, foams, etc. (Ref 2-4) that have been applied in a variety of engineering structures. Recently, with the functional requirement being increasingly high, a few novel EAM, including bioinspired polymers (Ref 5), shear-thickening liquids (STL) (Ref 6), and nanoporous materials functionalized (NMF) liquids (Ref 7-9), have drawn considerable attention. The bioinspired polymers work under tension, and the energy dissipation mechanism of STL is associated with shear deformation. Under a compressive loading, which is the primary working condition of many protective systems, NMF liquids offer high-energy dissipation effectiveness.

An NMF liquid consists of nanoporous particles immersed in a liquid phase. The nanopore surface must be nonwettable to the liquid. Thus, at rest, the nanopores would remain empty. As an external pressure is applied on the liquid phase, by forcing the liquid molecules into the nanopores, the nanopore surface comes into contact with liquid molecules, so that the system's free energy rises rapidly. The increase in system free energy can be given as

$$E = \Delta\gamma A \quad \text{(Eq 1)}$$

where $\Delta\gamma$ is the excess solid-liquid interfacial tension and A is the specific surface area. Typically, $\Delta\gamma$ is around 10 mJ/m^2 and A is 10^2 to 10^3 m^2/g. Thus, the energy density is at the level of 10 J/g, which is much larger than that of ordinary EAM.

In the past few years, a number of important characteristics of NMF liquids have been studied both experimentally and numerically. For instance, it has been noticed that gas nanophase plays a critical role in both liquid infiltration and defiltration (Ref 10, 11). The liquid composition, which can be controlled by adjusting liquid matrix (Ref 12) and admixtures (Ref 13, 14), also has a pronounced influence on the system performance. For many NMF liquids, once the liquid molecules are compressed into the nanopores, they would be "locked" inside; that is, when the external pressure is removed, the system volume would not recover. In other systems, the confined liquid phases are unstable. Upon unloading, they would decompose into gas phases and bulk liquid phases. As a result, the systems can work under cyclic loadings (Ref 15). In a few NMF liquids, the confined liquid phases may defiltrate immediately after the external pressure is lowered. These materials are of volume memory characteristics, having great potential for active control (Ref 16).

One question that remains unanswered is: what is the upper limit of the energy density of NMF liquids? As discussed above, the energy density increases with $\Delta\gamma$. To enhance the energy absorption performance, so that minimum amount of nanoporous material is needed to dissipate a specified amount of energy, materials of large surface areas and solid-liquid systems of high interfacial tensions must be used. If the liquid phase is water based, $\Delta\gamma$ is usually around 10 mJ/m^2. While a number of techniques, such as surface modification of nanoporous materials (Ref 17, 18) and adjustment of liquid composition (Ref 19), have been developed, the improvement is usually 20-50%. To achieve a higher interfacial tension, liquids of much larger surface energies, such as liquid metals, should be employed. In this article, we focus on the mechanical behaviors of NMF liquids. We attempt to estimate their maximum possible energy density, which provides a basis for material selection and structural optimization. The environmental,

This article was presented at Materials Science & Technology 2007, Automotive and Ground Vehicles symposium held September 16-20, 2007, in Detroit, MI.

Aijie Han, Venkata K. Punyamurtula, Taewan Kim, and **Yu Qiao**, Department of Structural Engineering, University of California – San Diego, La Jolla, CA 92093-0085. Contact e-mail: yqiao@ucsd.edu.

financial, and safety concerns are beyond the scope of the current study.

2. Experimental

In the current research, we investigated a nanoporous material of a large surface area, commonly known as mobil crystalline material (MCM) 41. By using a liquid metal, the value of both the interfacial tension and the nanopore surface area are close to the maximum possible values, so that the energy density represents the upper limit that can be reached using an NMF liquid. The network material was obtained from Sigma-Aldrich (CAT No. 643745). To increase the free energy of nanopore surface, the material was treated in a 2.5% dry toluene solution of chlorotrimethylsilane, followed by vacuum drying at 100 °C for 24 h. The treatment temperature was maintained at 20 °C for 10 min, with the mixture being stirred continuously, and then at 90 °C for 1 h, as the solution was refluxed. Then, the MCM41 was collected by vacuum filtering, washed in dry toluene and warm water, and vacuum-dried repeatedly. During the surface treatment, silane groups were formed at hydroxyl sites, modifying the nanopore surface structure (Ref 20). The surface-treated MCM41 was analyzed in a Tristar-3000 Gas Absorption Analyzer, and its nanopore surface area distribution is given in Fig. 1. The modal value and the average value of pore size were 2.4 and 3.5 nm, respectively. The specific surface area was 807 m^2/g, and the specific pore volume was 0.8 cm^3/g.

Mercury (Hg) was chosen as the liquid metal. About 0.2 g of MCM41 was sealed in a stainless steel cylinder, together with 5 cm^3 of mercury, as depicted in Fig. 2. Since the nanopore surface was nonwettable to Hg, at rest the nanopores would remain empty. By applying a quasi-static pressure through a piston, Hg atoms could be forced into the nanopores, and thus the system volume decreased considerably, as shown in Fig. 3. As the pressure reached the set point, the piston was moved out of the cylinder. Once the pressure was reduced to zero, the same loading procedure was repeated, and the system behavior at the second loading was observed. The maximum pressure varied from 160 to 300 MPa. As the maximum pressure increased, smaller nanopores were involved in the pressure-induced infiltration (PII), and thus the infiltration volume became larger. It was noticed that as the pressure exceeded 200 MPa, the infiltration volume was constant at 0.8 cm^3/g, indicating that nearly all the nanopore surface was exposed to the Hg phase. Under this condition, the system properties are summarized in Table 1.

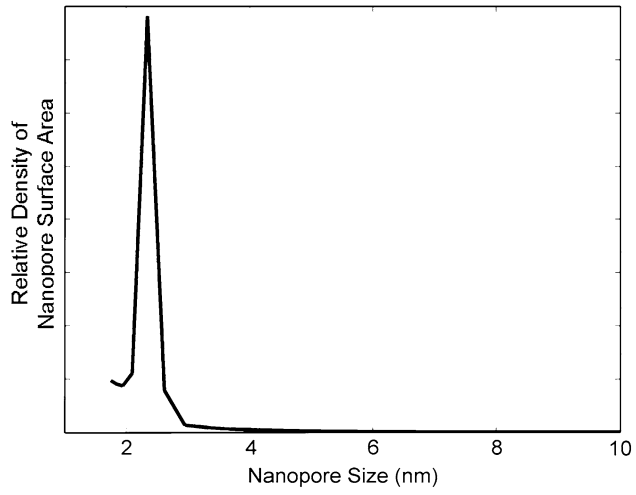

Fig. 1 The distribution of nanopore size

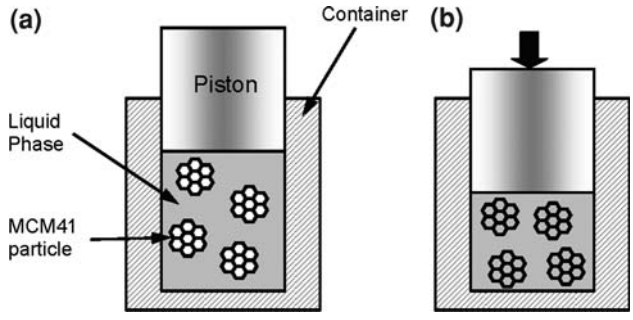

Fig. 2 The experimental setup: (a) prior to and (b) after the pressure-induced infiltration test

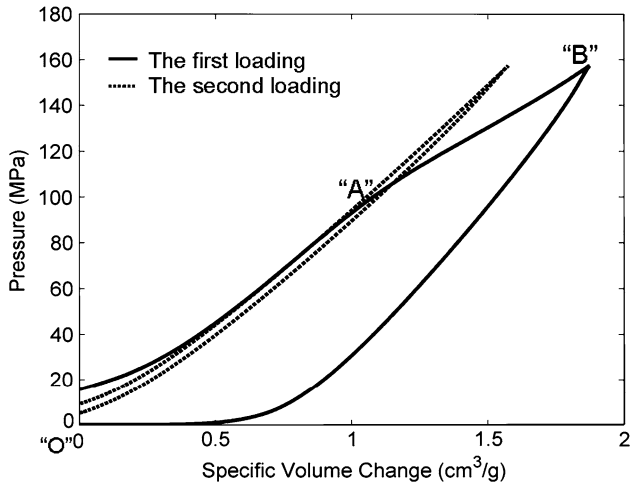

Fig. 3 Typical sorption isotherm curves. The maximum pressure is set to 160 MPa. The curves have been shifted along the horizontal axis so that the tangents of lower-pressure linear sections pass through the origin ("O")

Table 1 The infiltration behaviors of MCM41 with mercury

	Mass density, g/cm^3	Infiltration pressure, MPa	Effective porosity, cm^3/g	Energy dissipation effectiveness, J/g
The first loading cycle	0.4	102	0.8	140
The second loading cycle	11	104	0.05	4

3. Results and Discussion

Even at a relatively low pressure, the sorption isotherm curves shown in Fig. 3 are of finite slopes, which are primarily determined by the mechanical compliance of the experimental setup and the bulk modulus of mercury. When the pressure reached about 100 MPa (point "A" in Fig. 3), the slope abruptly reduces, indicating that the system compressibility becomes much larger. Clearly, as the capillary effect of nanopores is overcome, the liquid phase enters the empty space inside the MCM41 particles, and consequently the system volume decreases. The liquid infiltration does not take place in all the nanopores simultaneously. According to the classic Laplace-Young equation, the required infiltration pressure is

$$P_{\text{in}} = 4\Delta\gamma/d \qquad \text{(Eq 2)}$$

where d is the pore size. Thus, infiltration starts in the largest nanopores. Once these pores are filled, the pressure must be increased to a higher level to induce infiltration in smaller nanopores, which is indicated by the change in the slope of infiltration plateau ("AB") of the sorption isotherm curve. According to Fig. 1, the largest nanopore size is around 4 to 5 nm. Since at the onset of pressure-induced infiltration (point "A" in Fig. 3) the pressure P_{in} = 102 MPa, through Eq 2 it can be obtained that $\Delta\gamma \approx 128$ mJ/m^2, which is much higher than that of aqueous-solution-based systems (Ref 21).

As the peak pressure is reached and the piston is moved out of the cylinder, the unloading path is quite different from the loading path, causing a pronounced hysteresis. The slope of unloading path is similar to the slope in section "OA," which suggests that the confined mercury atoms do not defiltrate, even when the peak pressure is relatively low and the nanoporous space is only partly filled. That is, the compressed gas phase in an MCM41 particle cannot overcome the "self-locking" effect, which may be attributed to the "ink-bottle" effect associated with the irregular nanopore structure (Ref 22), the breakdown of gas nanobubbles (Ref 10), and/or the formation of new bonds between liquid molecules and nanopore walls (Ref 11). Since the interfacial tension cannot be released upon unloading, the mechanical work done by the loading path is effectively dissipated. As shown in Table 1, in the first loading cycle, the absorbed energy density is E = 140 J/g. This is the highest value that has been achieved by using NMF liquids. Since in the MCM41-Hg system the values of both the interfacial tension and the surface area are close to the maximum possible values of nanoporous processing technology, this highest value indicates the upper limit of system performance.

As the energy absorption capacity is fully utilized (i.e., when the maximum pressure is higher than 200 MPa), the specific infiltration volume, which is defined as the system volume decrease normalized by the mass of MCM41, is about 0.8 cm^3/g, nearly the same as the porosity measured in the gas absorption analysis. Therefore, the energy absorption should be achieved across the entire nanopore surface. According to Eq 1, $\Delta\gamma$ can be assessed as $\Delta\gamma = E/A$ = 173 mJ/m^2, comparable with but larger by 26% than the estimation based on the Laplace-Young equation, probably because of the sub-nm features at nanopore surfaces that make the assumption of circular nanopore cross section less relevant.

After the first loading-unloading cycle, the nanopores are filled with mercury; hence, when the external pressure is applied again, little infiltration can be observed. That is, energy absorption can be achieved only at the first loading, and such a system is suitable for one-time protection applications, such as car bumpers. Before the PII experiment, the MCM41 particles were white powders, with an average particle size of 50 μm and a density of 0.4 g/cm^3. The weight density is about five times smaller than that of bulk silica (2.1 g/cm^3), in agreement with the fact that the porosity is nearly 80%. After the PII experiment, the MCM41 particles form large aggregates, with a size of around 1-2 mm. The weight density largely increases to 11 g/cm^3. This clearly shows that the nanopores are filled with mercury. The effective density of the confined mercury is around 13 g/cm^3, nearly the same as the specific weight of bulk mercury, suggesting that the atomic structure of mercury phase in nanopores may be similar to that in bulk phase.

One can note that the MCM41-mercury system may not be directly useful to the industries due to cost and environmental concerns. Nevertheless, the current study gives the upper limit of the performance of NMF liquids. As long as the required energy absorption effectiveness is lower than 140 J/g, this technique is relevant; otherwise, new protection mechanisms must be discovered. It is envisioned that if other liquid metals, such as tin and gallium, are used, the system can be much more environment friendly.

4. Concluding Remarks

To assess the upper bound of energy density of NMF liquids, we investigated an MCM41-mercury system, in which the values of both the solid-liquid interfacial tension and the specific nanopore surface area are close to the maximum values that can be achieved by the current materials-processing technology. The energy absorption effectiveness is measured to be 140 J/g, representing the limit of the NMF liquid technique. As the external pressure is sufficiently high, most of the nanopores can be filled. The effective interface tension is 0.17 J/m^2. Little defiltration would take place even if the infiltration is incomplete. The effective weight density of confined mercury in nanopores is close to that of bulk phase.

Acknowledgment

This study was supported by The Army Research Office under Grant No. W911NF-05-1-0288.

References

1. G. Lu and T. Yu, *Energy Absorption of Structures and Materials*, CRC Press, 2003
2. M.S. Arzhakov, G.E. Zaikov, and S.A. Arzhakov, *Structural and Mechanical Behaviors of Polymers*, Nova Sci. Publ., 1997
3. K.K. Chawla, *Composite Materials*, Springer, 1998
4. D.J. Hartl and D.C. Lagoudas, Aerospace Applications of Shape Memory Alloys, *Proc. Inst. Mech. Eng. Pt. G-J. Aero. Eng.*, 2007, **221**, p 535–552
5. Z. Guan, Supermolecular Design in Biopolymers and Biomimetic Polymers for Properties, *Polym. Inter.*, 2007, **56**, p 467–473
6. M.J. Decker, C.J. Halbach, C.H. Nam, N.J. Wagner, and E.D. Wetzel, Stab Resistance of Shear Thickening Fluid Treated Fabrics, *Compos. Sci. Tech.*, 2007, **67**, p 565–578
7. F.B. Surani and Y. Qiao, An Energy Absorbing Polyelectrolyte Matrix Composite Material, *Compos. Pt. A*, 2006, **37**, p 1554–1556

8. F.B. Surani and Y. Qiao, Pressure Induced Liquid Infiltration in a Functionalized Poly(acrylic acid-co acrylamide) Potassium Salt Gel Matrix Material, *Mater. Res. Innov.*, 2006, **10**, p 129–137
9. F.B. Surani, X. Kong, D.B. Panchal, and Y. Qiao, Energy Absorption of a Nanoporous System Subjected to Dynamic Loadings, *Appl. Phys. Lett.*, 2005, **87**, p 163111
10. A. Han, X. Kong, and Y. Qiao, Pressure Induced Infiltration in Nanopores, *J. Appl. Phys.*, 2006, **100**, p 014308
11. Y. Qiao, G. Cao, and X. Chen, Effects of Gas Molecules on Nanofluidic Behaviors, *J. Am. Chem. Soc.*, 2007, **129**, p 2355–2359
12. V.K. Punyamurtula, A. Han, and Y. Qiao, Damping Properties of Nanoporous Carbon – Cyclohexane Mixtures, *Adv. Eng. Mater.*, 2007, **9**, p 209–211
13. X. Kong, F.B. Surani, and Y. Qiao, Energy Absorption of Nanoporous Silica Particles in Aqueous Solutions of Sodium Chloride, *Phys. Scripta*, 2006, **74**, p 531–534
14. A. Han and Y. Qiao, Pressure Induced Infiltration of Aqueous Solutions of Multiple Promoters in a Nanoporous Silica, *J. Am. Chem. Soc.*, 2006, **128**, p 10346–10349
15. X. Kong and Y. Qiao, Improvement of Recoverability of a Nanoporous Energy Absorption System by Using Chemical Admixtures, *Appl. Phys. Lett.*, 2005, **86**, p 151919
16. A. Han and Y. Qiao, A Volume Memory Liquid, *Appl. Phys. Lett.*, 2007, **91**, p 173123
17. A. Han and Y. Qiao, Effects of Surface Treatment of a MCM-41 on Motions of Confined Liquids, *J. Phys. D-Appl. Phys.*, 2007, **40**, p 5743–5746
18. A. Han and Y. Qiao, Controlling Infiltration Pressure of a Nanoporous Silica Gel via Surface Treatment, *Chem. Lett.*, 2007, **36**, p 882–883
19. A. Han and Y. Qiao, Infiltration Pressure of a Nanoporous Liquid Spring Modified by an Electrolyte, *J. Mater. Res.*, 2007, **22**, p 644–648
20. M.H. Lim and A. Stein, Comparative Studies of Grafting and Direct Syntheses of Inorganic-Organic Hybrid Mesoporous Materials, *Chem. Mater.*, 1999, **11**, p 3285–3295
21. X. Kong and Y. Qiao, Thermal Effects on Pressure Induced Infiltration of a Nanoporous System, *Phil. Mag. Lett.*, 2005, **85**, p 331–337
22. G.T. Shaw, *Porosimetry by Mercury Injection*. Dept. of Mines and Technical Surveys, Mines Branch, 1963